European Neuropsychopharmacology (2010) **20**, 96–111

www.elsevier.com/locate/euroneuro

A mouse model of anxiety molecularly characterized by altered protein networks in the brain proteome

Éva M. Szegő [a,b,1], Tamás Janáky [b], Zoltán Szabó [b], Attila Csorba [b], Hajnalka Kompagne [c], Géza Müller [c], György Lévay [c], Attila Simor [a,b], Gábor Juhász [a], Katalin A. Kékesi [a,d,*]

[a] *Laboratory of Proteomics, Institute of Biology, Eötvös Loránd University, Budapest, Pázmány P. stny. 1/c, H-1117, Hungary*
[b] *Institute of Medical Chemistry, University of Szeged, Szeged, Dóm tér 8, H-6720, Hungary*
[c] *EGIS Pharmaceuticals Plc, Budapest, Bökényföldi út 116-120, H-1165, Hungary*
[d] *Department of Physiology and Neurobiology, Eötvös Loránd University, Budapest, Pázmány P. stny. 1/c, H-1117, Hungary*

Received 22 July 2009; received in revised form 25 September 2009; accepted 12 November 2009

KEYWORDS
Anxiety;
Drug discovery;
Molecular characterization;
Mouse model;
Protein interaction networks;
Proteomics

Abstract

Recently, several attempts have been made to describe changes related to certain anxiety states in the proteome of experimental animal models. However, these studies are restricted by limitations regarding the number and correct identification of separated proteins. Moreover, the application of a systems biology approach to discover the molecular mechanisms of anxiety requires genetically homogenous inbred animal models. Therefore, we developed a novel mouse model of anxiety using a combination of crossbreeding (inbred for 35 generations) and behavioral selection. We found significant changes in 82 proteins in the total brain proteome compared to the control proteome. Thirty-four of these proteins had been previously identified in other anxiety, depression or repeated psychosocial stress studies. The identified proteins are associated with different cellular functions, including synaptic transmission, metabolism, proteolysis, protein biosynthesis and folding, cytoskeletal proteins, brain development and neurogenesis, oxidative stress, signal transduction. Our proteomics data suggest that alterations in serotonin receptor-associated proteins, in the carbohydrate metabolism, in the cellular redox system and in synaptic docking are all involved in anxiety.

1. Introduction

The main criticism against recent mood disorder therapy is that available treatments target the symptoms rather than the underlying molecular mechanisms responsible for the disease. One of the reasons for this is that the mechanisms are barely known (Agid et al., 2007). Animal models for

* Corresponding author. Laboratory of Proteomics, Institute of Biology, Eötvös Loránd University, Budapest, Pázmány P. stny. 1/c, H-1117, Hungary. Tel./fax: +36 1 3812204.
E-mail address: kakekesi@dec001.geobio.elte.hu (K.A. Kékesi).
[1] Present address: Department of Neurodegeneration and Restorative Research, Georg-August University, DFG Research Center: Molecular Physiology of the Brain (CMPB), Göttingen, Waldweg 33, D-37073, Germany.

0924-977X/$ - see front matter © 2009 Elsevier B.V. and ECNP. All rights reserved.
doi:10.1016/j.euroneuro.2009.11.003

human mood disorders have been developed on the basis of altered stress reaction in some experimental stress situations, and these represent simplified models of the human diseases (Sousa et al., 2000; Borsini et al., 2002; Pawlak et al., 2003; Kalueff and Murphy, 2007). In addition, human psychiatric disorders are frequently loosely diagnosed on the bases of behavioral symptoms rather than pathological molecular mechanisms, while the prescribed drugs bind to certain target molecules (Abi-Dargham et al., 1997; Bourin and Hascoet, 2001). It is clear that one of the major problems in psychiatric research today is the fact that our knowledge of the molecular mechanisms of psychiatric disorders is limited (Agid et al., 2007).

The development of medications for anxiety disorders has also been a serendipitous process, as early anxiolytic agents acted on a limited number of amino acid and monoamine receptors (Uys et al., 2006). Years of experimentation using traditional biochemical approaches have proved the role of the serotonin receptor malfunctions in anxiety (Handley and McBlane, 1993; Graeff et al., 1996), and advances in cellular biology have led to a shift in focus from such receptors to intracellular signaling pathways (Bachmann et al., 2005; Zarate et al., 2006).

A growing amount of evidence demonstrates that agents used in the treatment of anxiety disorders alter the rat brain proteome after chronic administration (Khawaja et al., 2004; Carboni et al., 2006b; Bayés and Grant, 2009) and there are several altered proteins associated with various cellular functions that changed after repeated psychosocial stress (Carboni et al., 2006a). Recently, enolase–phosphatase was identified as a biomarker in a proteomics study of an anxiety trait from a mouse model (Ditzen et al., 2009), which provides support to the idea that a proteomics-based phenotyping of anxiety mouse models is a realistic undertaking.

Strategies for breeding anxiety models include selection of extreme individuals within a population that have abnormal stress reactions to a variety of behavioral tests, such as the forced swimming and the elevated plus maze tests (Kalueff and Murphy, 2007). These methods result in small groups of animals that have some similarities in phenotype and heterogeneous genomes. Another method involves crossbreeding of stress-sensitive animals. This results in an anxiety model strain that has good heredity of the behavioral symptoms of anxiety (Bourin et al., 2007), similarities in phenotype and a relatively homogenous genome. The high resolution and sensitivity of gene chipping and proteomics require groups of animal that are genetically as homogenous as possible to allow experiments aiming at drug discovery. We report here an inbred anxiety model (AX) mouse strain that we validated with the combination of genetic and behavioral selection strategies for proteomics studies by determining the differences in its brain proteome from that of the normally behaving source strain. A two-dimensional differential gel electrophoresis (DIGE)-based proteomics study was performed in order to reveal the differences in brain tissue phenotypes between normal, non-anxious (NAX) and anxiety model mice. We could confirm several protein alterations that were already known from the literature of anxiety and depression, such as inflammatory cytokines or synaptic density proteins (Miller and O'Callaghan, 2005; Hahn et al., 2009), therefore we could estimate the extent of reproducibility of known molecular mechanisms in our model.

In addition to compiling a list of the altered proteins, we performed functional clustering and further functional network modeling of the most interesting groups of anxiety-modulated proteins in order to provide data that could describe the putative molecular mechanisms involved in anxiety. We report here a reliable workflow for molecular characterization of animal models of psychiatric disorders. This approach can also estimate the coverage of those molecular mechanisms in an animal model that are known in a human disease. Moreover, our data suggest synaptic and cellular structure proteins as putative new targets for studies on psychiatric illnesses.

2. Experimental procedures

2.1. Animal care and handling

We used 36 mice for behavioral tests, and 12 mice for proteomics experiments. Animal handling and experimentation conformed to the Council Directive 86/609/EEC, the Hungarian Act of Animal Care and Experimentation (1998, XXVIII) and local regulations for the care and use of animals for research.

2.2. Development of anxiety (AX) mouse strain

We developed two inbred mouse strains. Our aim was to produce one strain (AX) that would be more anxious than wild-type mice, and the other strain (NAX) that would display a normal to slightly reduced anxiety state under behavioral test conditions. Individuals of a non-commercially available inbred mouse strain (MG15) were maintained at EGIS Pharmaceuticals Co. (Budapest, Hungary) to study skeletal muscle development. Mice from MG15 strain were crossed with NMRI mice (Charles River Ltd., Budapest, Hungary). Twenty-five to thirty individuals of the initial population (21 days old) were placed in a large cage. They were selected by gender and labeled individually. At the age of 35–42 days, we moved the mice to new cages twice a week. Selection was made on the basis of anticipatory anxiety behavior during the handling procedure. Mice approaching the experimenter's hand were separated from those that never volunteered to be handled. Later on these two groups were inbred for four generations and it was confirmed that mice derived from the early group were always handled early while those that tried to avoid handling were always moved later. The two groups of mice displayed markedly different behavior. We marked the first group as non-anxious (NAX) and the second group as anxious (AX) mice. By decreasing the number of families and crossing brothers and sisters from the same litter, we achieved an inbred strain series. The present work was performed on NAX and AX mice that were inbred through 35 generations.

2.3. Behavioral tests

Experiments were performed on 22 male mice at the age of 15–17 weeks (NAX: $n=12$; AX: $n=10$). We used three behavioral models to characterize the mice, namely open-field activity, elevated plus maze and light–dark tests. There was a 3–4-day interval between experiments.

2.3.1. Open-field test

Locomotor activity was measured in automated open-field arenas by interruptions of horizontal and vertical infrared beams. Beam interruptions were counted by an Omnitech Animal Activity Monitor. The arenas were open-topped 41×41×30 cm plastic boxes. The test

room was dimly illuminated using indirect light. Animals were habituated to the test room for 30 min before the experiments. They were then placed individually in the centre of the arena and left there for 15 min. Horizontal activity, distance traveled, time spent in the central zone of the arena and immobile time were measured.

2.3.2. Elevated plus maze test

The equipment was made of black-painted wood and consisted of 2 opened (25×8 cm) and 2 closed arms (25×8×20 cm) with a central zone of 8×8 cm. The maze was elevated to 60 cm. Behavior on the maze was recorded by an experienced person through a CC video system. The room was dimly illuminated by a cross-shaped lamp above the maze. Mice were habituated to the test room for 30 min before the experiments. Animals were placed individually in the central zone of the plus maze in a random order, and they were left to explore the maze for 5 min, after which they were returned to their home cages.

2.3.3. Light–dark test

The setup consisted of Plexiglas cages (41×41×30 cm) that were separated into two compartments. The opened compartment was open-topped, made of transparent Plexiglas and brightly illuminated by a 60 W light bulb. The dark compartment was made of black Plexiglas and was covered with a top. The two compartments were connected by a small 6×6 cm gate. Activity was measured automatically by interruptions of horizontal and vertical infrared beams. Mice were individually placed in the centre of the opened compartment, facing away from the partition and allowed to explore the apparatus for 5 min. The number of light–dark transitions, time spent in the light compartment and movement time in either compartment were recorded.

2.4. Statistics for the behavioral tests

We applied a parametric test (two-sample *t*-test), when the distribution of the data was normal, and the standard deviations of the NAX and AX groups were homogenous (open-field, light–dark tests), while the non-parametric Mann–Whitney test was used for the elevated plus maze test.

2.5. Sample preparation and fluorescence two-dimensional differential in-gel electrophoresis (2D-DIGE)

Mice were sacrificed with cervical dislocation, and brains were quickly removed from the skull. We removed the cerebellum, brainstem and the olfactory bulb, and we stored the samples at −80 °C until use. Samples were mechanically homogenized in lyses buffer (7 M urea, 2 M thiourea, 4% CHAPS, 20 mM Tris, 5 mM magnesium-acetate, at pH 8.5, Protease Inhibitor Mix, 1:1000), then sonicated and centrifuged for 1 h at 14,000 ×*g* at 4 °C. The pH of the supernatant was adjusted to 8.5 and protein concentration of the sample was measured by PlusOne Quant Kit (GE Healthcare). The protein content was between 4 and 10 μg/μl. Samples of 50 μg were labeled with CyDye DIGE Fluor Minimal Labeling Kit (GE Healthcare) at a concentration of 400 pmol/50 μg protein. Brain lysates from AX or NAX mice were labeled with Cy3 and Cy5 randomly, and the reference (pooled internal standard, from AX and NAX lysates) labeled with Cy2. Labeled proteins were dissolved in isoelectric focusing (IEF) buffer containing ampholytes (0.5 v/v %), DTT (0.5 m/v %), 8 M urea, 30% glycerine, 2% CHAPS, and rehydrated passively onto 24 cm IPG strips (pH 3–10 NL, GE Healthcare) for at least 14 h at room temperature. After rehydration, the IPG strips were subjected to first dimension IEF for 24 h to attain a total of 80 kV h. Focused proteins were first reduced by equilibrating with buffer containing 1% (w/v) mercaptoethanol for 20 min and then alkylated with a buffer containing 2.5% (w/v) iodoacetamide for 20 min. After reduction and alkylation, the IPG strips were loaded onto 10% polyacrylamide gels (24×20 cm), and SDS-PAGE was conducted at 10 W/gel. Following electrophoresis, gels were scanned in a TyphoonTRIO+ scanner (GE Healthcare) using appropriate lasers and filters with the PMT biased at 580 V. Images in different channels were overlaid using selected colors and differences were visualized using Image Quant software (GE Healthcare). Differential protein analysis was performed using DeCyder software package, DIA and BVA modules (GE Healthcare). For the identification of proteins in spots of interest, preparative 2D electrophoresis was performed separately using a total of 800 μg of proteins per gel. Resolved protein spots were visualized by Colloidal Coomassie Blue G-250. Individual spots were excised from the gel, destained, and subjected to in-gel digestion with trypsin for 24 h at 37 °C (Shevchenko et al., 1996). Tryptic peptides were extracted from gel pieces using 5% formic acid and were dried under vacuum. Six analytical and two preparative gels were run in the experiment.

2.6. Protein identification

All LC–MS experiments were performed using Agilent 1100 Series nano-LC coupled through an orthogonal nanospray ion source to an Agilent LC–MSD XCT Plus ion trap mass spectrometer (Agilent Co., USA). The nano-LC system was operated in sample enrichment/desalting mode using a ZORBAX 300SB-C18 enrichment column (0.3×50 mm, 5 μm), and for the chromatography we used ZORBAX 300 SB-C18 (75 μm×150 mm) nanocolumn. Elution of peptides was accomplished by gradient elution at a flow rate of 300 nl/min with a gradient from 100% solvent A (0.1% formic acid in water) to 40% solvent B (0.1% formic acid in acetonitrile) in 25 min. MS was operated in peptide scan auto-MS/MS mode, acquiring a full-scan MS spectra (300–1600 *m/z*) at a scan speed of 8100 u/s and a resolution of less than 0.35 u (FWHM). From the four most abundant peaks in the MS spectrum, automated, data-dependent MS/MS was used to collect MS/MS spectra (100–1800 *m/z* at 26,000 u/s and a resolution of less than 0.6 u, FWHM).

All acquired data were processed and peak lists were generated by the Agilent DataAnalysis 3.2 software using default settings. All MS/MS samples were analyzed using Mascot 2.2.04 (Matrix Science, London, UK) and X! Tandem (www.thegpm.org; version 2007.01.01.1). Mascot and X! Tandem were set up to search the Swissprot 56.8 database (2009.02.10 release, 410,518 entries) assuming the digestion enzyme trypsin. Both search engines searched assuming a fragment ion mass tolerance of 0.80 Da and a parent ion tolerance of 1.5 Da. Iodoacetamide derivative of cysteine as a fixed modification and oxidation of methionine as a variable modification were specified in Mascot and in X! Tandem.

Scaffold (version Scaffold_2_02_03, Proteome Software Inc., Portland, OR) was used to validate MS/MS based peptide and protein identifications. Peptide identifications were accepted if they could be established at greater than 95.0% probability, protein identifications were accepted with greater than 95.0% probability and contained at least 2 identified peptides.

3. Results

3.1. Behavioral tests

Animals that were used in behavioral tests were selected from the same lines and same age as those that were used in the proteomics study. The results of the three behavioral tests were as follows.

3.1.1. Open-field test

In terms of horizontal activity, NAX animals were significantly more active than AX animals (Fig. 1, Panel A, $p<0.01$) and spent significantly longer time in the central zone (Fig. 1 Panel B, $p<0.01$) than AX animals. In addition, the AX animals spent more time in an immobile state than NAX mice

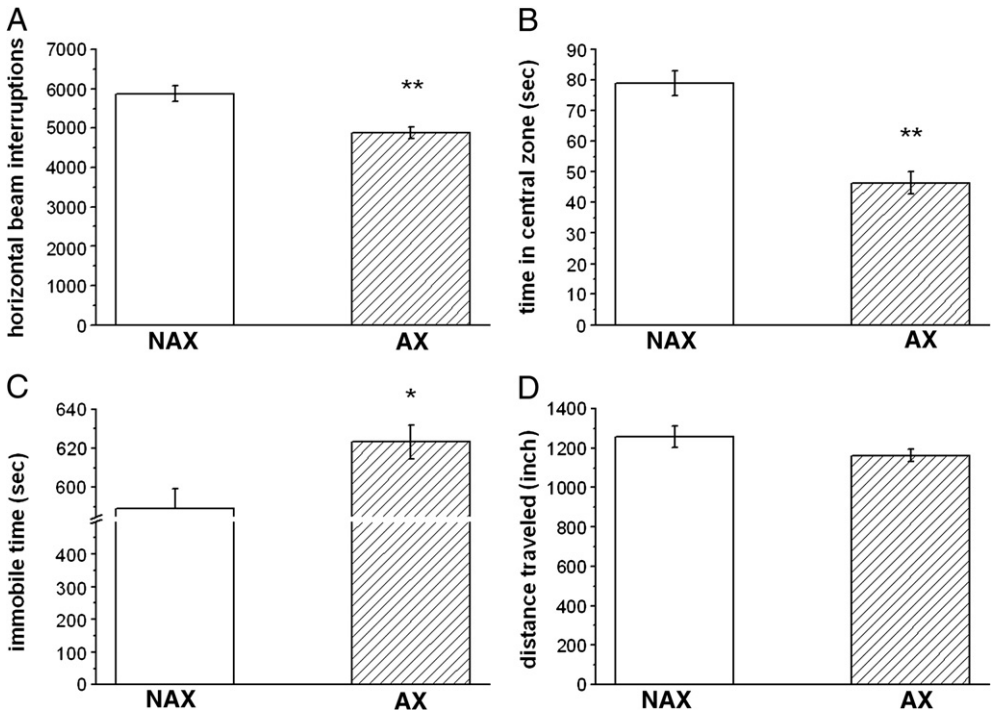

Figure 1 Behavioral parameters of non-anxious (NAX) and anxious (AX) mice in the open field. A: Horizontal beam interruptions; B: time spent in the central area; C: time spent in immobile state; D: distance traveled. *$p<0.05$, **$p<0.01$.

(Fig. 1, Panel C, $p<0.05$). On the other hand, when the distance traveled was examined, no significant difference was found between the groups, which reflected the absence of difference in locomotor activity. Time spent in the central zone of the arena was indicated 'fear' rather than activity.

3.1.2. Elevated plus maze test

The NAX animals tended to enter the open arms more frequently and stayed there longer ($p<0.01$ for open time and $p<0.01$ for open entries, Fig. 2). The number of total entries into the arms from the central zone for the NAX group

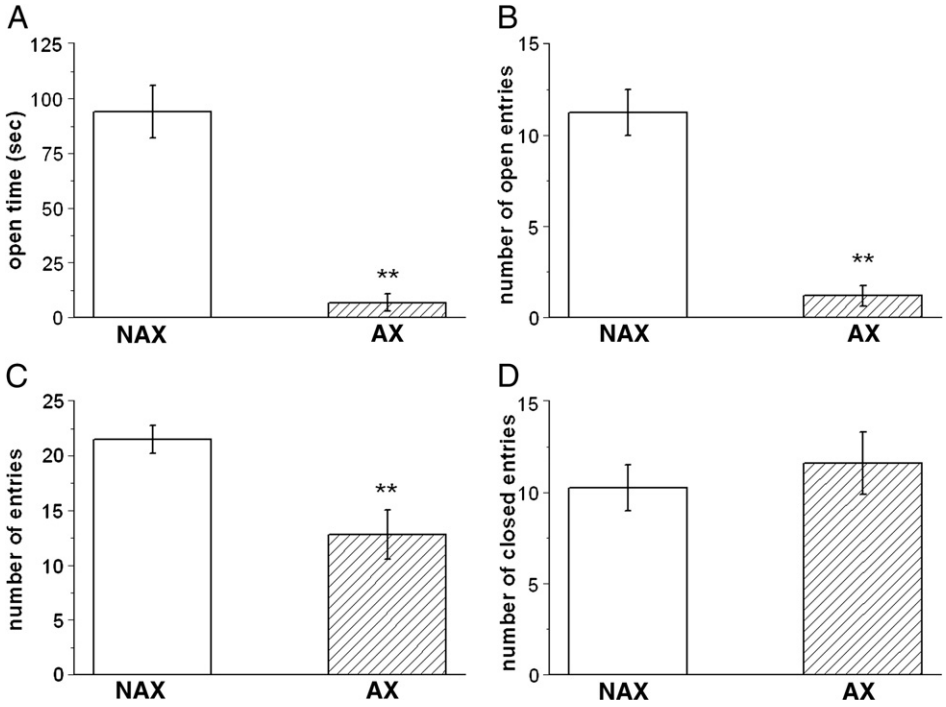

Figure 2 Behavioral parameters of non-anxious (NAX) and anxious (AX) mice in the elevated plus maze. A: Time spent in the open arms; B: number of open arm entries; C: total number of entries; D: number of closed arm entries. **$p<0.01$.

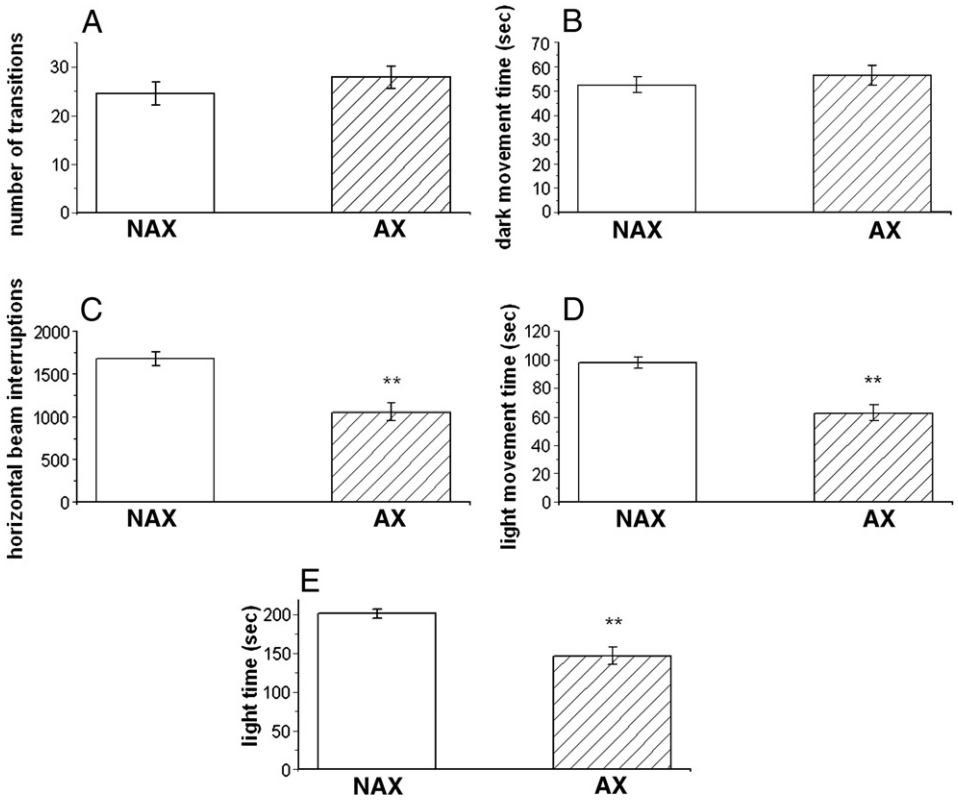

Figure 3 Behavioral parameters of non-anxious (NAX) and anxious (AX) mice in the light–dark box. A: Number of transitions between compartments, B: movement time in the dark compartment; C: number of horizontal beam interruptions, D: movement time in the light compartment, E: time spent in the light compartment. $^{**}p<0.01$.

was also significantly higher than that for the AX group ($p=0.0076$), but this difference was due to the extended number of open entries since the average number of closed entries for the two groups was almost equal (NAX = 10.25, AX = 11.6).

3.1.3. Light–dark test

The outcome was very similar to the results of other behavioral tests (Fig. 3). The movement time in the light compartment and the time spent in the light compartment were found to be significantly different between the two groups. The NAX animals spent more time and were more active in the light zone than the AX mice $p<0.01$ for movement time in the light compartment and $p<0.01$ for light time. On the other hand, there was no difference between the groups with regard to movement time in the dark compartment $p=0.464$ and the number of light–dark transitions $p=0.328$. This suggests that AX animals are more fearful in the aversive situation (the brightly illuminated box) than the NAX mice and that the decrease of moving time is not due to a reduced locomotor activity.

3.2. Altered proteins in AX mice

The proteomics data revealed that 82 proteins showed significantly different concentrations in the anxiety strain mice ($p<0.05$, $n=66$group) and 31 out of that 82 proteins are already known to be involved in mood disorders, particularly in anxiety and depression (Fig. 4 shows a representative gel image). In most of the publications, the same behavioral tests that we used here were applied. It should be noted that only NCBI Medline was used for the literature search, therefore involvement of additional proteins in anxiety cannot be excluded. All the proteins that were significantly altered in the AX strain are shown in Table 1.

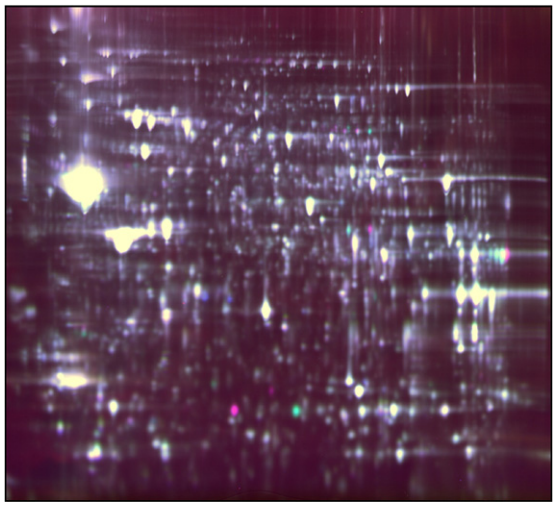

Figure 4 Representative gel image. The first dimension was carried out in pH 3–10 NL IPG strip and the second dimension was 24×20 cm SDS-PAGE.

3.3. Functional protein network

Proteins were sorted into eleven functional groups (Table 1) including synaptic transmission, carbohydrate metabolism, amino acid metabolism and proteolysis, nucleotide metabolism, haem and lipid metabolism, protein biosynthesis and folding, cytoskeletal proteins, brain development and neurogenesis, oxidative stress, and signal transduction. We also found 15 proteins that cannot be sorted into functional groups (miscellaneous). Functional networks were created for the altered proteins using the Ariadne Genomics Pathway Studio 6.1 software environment. We used the non-linear literature processing (NLP) literature search engine for creating networks, and the results were manually validated by reading full text publications. A synaptic docking protein network is shown in Fig. 5. Networks of other protein groups (e.g. metabolic pathways, oxidative stress) can be found on our website (http://proteom.elte.hu/networks). We found an extensive change in protein expression pattern, a down-regulation in signal transduction and changes in gene transcription factors (Table 1). There were specific alterations in carbohydrate metabolism, which is an important and very sensitive function of nerve cells (Table 1) (Sünram-Lea et al., 2008). Amino acid metabolism was also altered in the brain including metabolism of glutamate (Table 1). An important finding in our mouse strain is that the synaptic protein structure that is responsible for docking is altered in AX mice (Fig. 5). Modifications in the concentrations of cytoskeletal proteins (Table 1) in conjunction with altered synaptic docking proteins are remarkably novel aspects of anxiety-induced changes in the brain.

4. Discussion

We developed a mouse model of anxiety for use in drug discovery by combining behavioral selection with inbreeding. The novelty in our approach is that we characterized the anxiety phenotype of the strain by using proteomic techniques. This denotes a significant improvement because – although behavioral models of psychiatric disorders are no direct equivalents but analogous to the human diseases – successes in drug discovery suggest that even rodent models reproduce several molecular events of the human diseases (Bourin et al., 2007). We aimed to reproduce and considerably extend the already known molecular mechanisms. The frequently required molecular and biochemical homogeneity of the model was also indicated by the whole-brain proteome modification pattern in our study. It should be noted that although the DIGE method can only detect the most abundant 10–15% of proteins in a cell, the detected 2000–4000 proteins suitably characterize the phenotype of an animal model.

Even granting detection limit problems, we found 82 altered proteins, 31 of which had been previously identified in anxiety or depression studies (Table 1). Some of the 31 proteins are associated with serotonergic neurotransmission, for example eukaryotic translation initiation factor 4E (EIF4E), dynamin 1 (DNM1) and postsynaptic density protein-95 (PSD-95). According to the protein interaction databases, serotonin1B, 2C, and 5A receptors (HTR1B, HTR2C and HTR5A) are associated with processes in anxiety. We also report here 51 proteins still unknown in anxiety literature. They open either new targets for research or indicate molecular differences between animal models and human disease, a distinction that is the subject for further research. We also demonstrated that DIGE proteomics is a useful method for molecular characterization of an anxiety mice model. It should be noted, however, that both anxiety and depression literature were equally used for estimation of already known protein mechanisms of the anxiety disorder since several patients with different diseases share common symptoms (Martinowich et al., 2007).

4.1. Functional interpretation

We revealed that anxiety in mice induces an extensive change in the whole-brain proteome, including metabolic, gene expression, signaling and synaptic communication proteins. Glyoxalase, which detoxifies decarbonyl metabolites, participating in enzymatic defense against dicarbonyl stress and glycation, increases in low-anxiety models and decreases in high-anxiety models (Krömer et al., 2005). Therefore glyoxalase was suggested as a molecular biomarker in animal models (Ditzen et al., 2006, 2009); the decreased level of glyoxalase in our AX mice strain supports that it is probably a high-anxiety model. Several other pharmacologically interesting protein changes were reconfirmed in our studies: the peroxide proteins involved in redox reactions (Kishida and Klann, 2007) and free radical elimination like peroxiredoxin and some proteins of the signaling pathways (Wu et al., 2008), like mitogen activated protein kinase 6 (MAPK6) are supported (Pawlak et al., 2003; Duman et al., 2008).

Proteins coupled to serotonin or serotonin receptor were also changed in our model. EIF4E, which is a serotonin controlled protein (Carroll et al., 2006), decreased in AX mice as did also DNM1, a protein involved in vesicle recycling and the pathomechanisms of psychiatric diseases (Otomo et al., 2008). The level of postsynaptic density protein-95 is changed in the proteome of AX mice. A large body of literature regarding this integral membrane protein binding protein point to its role in several brain diseases, namely receptor anchoring via PDZ domains (including serotonin receptors) and synaptic plasticity (Fernández et al., 2009; Hahn et al., 2009; Gisler et al., 2008; van Zundert et al., 2004). An immense amount of literature is available on serotonergic transmission in psychiatric disorders (Wand, 2005). Thus, our model gives further evidence that the serotonergic system is involved in the control of anxiety. However, the number and connection of serotonin-related proteins were far less than the expected values. Probably this was a consequence of using whole-brain tissue rather than synaptosomes from anxiety-related brain areas, the former having masked structure and cell compartment specific changes in the proteome.

We also observed protein changes unmentioned in anxiety literature. We found altered proteins in the synaptic docking mechanism and some structural elements of the cytoskeleton, as indicated by an increased level of ezrin (Lowry et al., 2008), or decreased expression of capping protein (actin filament) muscle Z-line, alpha 2 protein CAPZA2 (Scoles, 2008). Changes in the structural proteins in brain cells can be particularly interesting, because these proteins are involved in synaptic plasticity or molecular tuning of synapses (Holtmaat and Svoboda, 2009). The altered group of docking

Table 1 Protein differences between non-anxious (NAX) and anxious (AX) mice arranged in functional clusters. Abbreviations: M — models (animal, cell culture) and HD — human disorders.

Gene name	Protein name	Spot no.	Accession no.	*p*-value	Fold change	MW	Seq. coverage	Cellular localization	Function	Reference (anxiety or depression)
Synaptic transmission										
ACTR1A	ARP1 actin-related protein 1 homolog A, centractin alpha (yeast)	2033	P85970, Q9CVB6	0.0021	1.48	42,957	26.3	Cytoplasm	Synaptosomal patterning, growth cone development	
ATP6V1E1	ATPase, H+ transporting, lysosomal 31 kDa, V1 subunit E1	2895	P50518, Q6PCU2	0.045	−1.05	31,729	35.6	Cytoplasm, mitochondria	Synaptic vesicle proton gradient generation	(Al-Damluji, 2004)
GDI2	GDP dissociation inhibitor 2	1870	P50399	0.01	1.06	50,521	34.6	Cytosol, Golgi apparatus	Regulation of membrane trafficking	
LIN7A	lin-7 homolog A (*C. elegans*)	3196	Q8JZS0, Q9Z250	0.04	1.26	25,845	29.7	Membrane, synaptosoma	Synaptic vesicle transport	
PSD-95	Postsynaptic density protein-95	827	Q62108	0.0004	1.18	80,456	14.1	Cytoplasm, plasma membrane	Synaptic transmission, neurogenesis, learning	(Toro and Deakin, 2005) HD
SYN2	Synapsin II	1060	Q64332	3.80E−06	4.04	63,355	14	Plasma membrane, synaptosoma	Synaptic vesicle membrane	
Carbohydrate metabolism										
ENO1	Enolase 1, (alpha)	1801	P17182	0.046	1.05	47,124	48.4	Cytoplasm, nucleus, plasma membrane	Glycolysis	
G6PD	Glucose-6-phosphate dehydrogenase	1419	Q00612	0.011	1.06	59,245	49.5	Cytoplasm, endoplasmic reticulum, nucleus	Glucose metabolism	
LDHB	Lactate dehydrogenase B	2779	P16125	0.0063	−1.12	36,595	34.7	Cytoplasm	Anaerobic glycolysis	(Johnson et al., 2008) HD
MDH1	Malate dehydrogenase 1, NAD (soluble)	2456	O88989, P14152	0.016	−1.1	36,466	19.2	Cytosol	Carbohydrate metabolism	(Beasley et al., 2006) HD
NDUFS1	NADH dehydrogenase (ubiquinone) Fe–S protein 1	693	Q91VD9	0.012	1.17	79,731	18.8	Mitochondria	Electron transport	
PDHA1	Pyruvate dehydrogenase (lipoamide) alpha 1	2033	P26284, P35486	0.0021	1.48	43,209	23.6	Extracellular space, mitochondria	Conversion of pyruvate to acetyl-CoA and CO_2	
PDHX	Pyruvate dehydrogenase complex, component X	1614	Q8BKZ9	0.015	1.21	49,182	27.4	Mitochondria	Glycolysis	(Khawaja et al., 2004) M
PGAM1	Phosphoglycerate mutase 1 (brain)	3157	P25113, Q9DBJ1	0.041	1.12	28,814	72.8	Cytoplasm	Carbohydrate metabolism	(King et al., 2009; Tohda et al., 2009; Ackermann et al., 2008; Tyeryar and Undie, 2007; Tyeryar et al., 2008) M
PKM2	Pyruvate kinase, muscle	1280	P52480	0.0019	2.47	57,827	40.3	Cytoplasm, mitochondria	Glycolysis	

SDHA	Succinate dehydrogenase complex, subunit A, flavoprotein (Fp)	1004	Q8K2B3	0.01	1.16	72,567	30.6	Mitochondria, membrane	Carbohydrate metabolism	
TKT	Transketolase (Wernicke–Korsakoff syndrome)	1051	P40142	0.018	1.07	67,614	14.1	Endoplasmatic reticulum, peroxisome	Regulation of growth	
UQCRC1	Ubiquinol-cytochrome c reductase core protein I	1842	Q9CZ13	0.0087	1.09	52,750	38.3	Mitochondria	Mitochondrial electron transport	(Johnston-Wilson et al., 2000; Nishikawa et al., 2008) M/HD
Amino acid metabolism										
ALDH6A1	Aldehyde dehydrogenase 6 family, member A1	1511	Q9EQ20	0.0059	1.08	57,898	45.4	Mitochondria	Amino acid metabolism	
GLO1	Glyoxalase I	3374	Q9CPU0	0.0045	1.41	20,793	48.9	Cytoplasm	Metabolism, detoxification of methylglyoxal	(Ditzen et al., 2006; Hovatta et al., 2005) M
GLUD1	Glutamate dehydrogenase 1	1615	P26443	0.0091	1.05	61,320	51.3	Mitochondria	Glutamate metabolism	(Beasley et al., 2006; Weder, 1978) M/HD
GLUL	Glutamate-ammonia ligase (glutamine synthetase)	2173	P15105	2.5E−05	−1.24	42,102	38.1	Cytoplasm, mitochondria	Glutamine metabolism	(Choudary et al., 2005; Garner et al., 2009; Garcia-Garcia et al., 2009; Cabral et al., 2009) M/HD
GOT2	Glutamic–oxaloacetic transaminase 2	2272	P05202	0.00049	−1.48	47,394	14.9	Mitochondria	Glutamate metabolism	(Covault et al., 2004) HD
WARS	Tryptophanyl-tRNA synthetase	1666	P32921	0.0094	1.05	54,341	53	Cytoplasm	Trna aminoacylation for protein translation	
YARS	Tyrosyl-tRNA synthetase	1348	Q91WQ3	0.016	1.09	59,088	50	Cytoplasm	Trna aminoacylation for protein translation	
Proteolysis										
ddx56	CNDP dipeptidase 2 (metallopeptidase M20 family)	1618	Q9D1A2	0.0039	−1.12	52,750	51.8	Cytosol	Carnosine and other dipeptide hydrolysis	
LONP1	lon peptidase 1, mitochondrial	2779	Q8CGK3	0.0063	−1.12	36,595	34.7	Mitochondria	Protein metabolism	
NLN	Neurolysin (metallopeptidase M3 family)	789	Q91YP2	0.0016	1.19	80,413	6.25	Cytoplasm, mitochondria	Proteolysis and peptidolysis	
NSF	N-ethylmaleimide-sensitive factor	715	P46460	0.02	1.12	82,599	16.5	Cytoplasm	Protein transport, proteolysis and peptidolysis	
PSMA6	Proteasome (prosome, macropain) subunit, alpha type, 6	3231	Q9QUM9	0.014	1.14	27,354	38.6	Cytosol, nucleus	Ubiquitin-dependent protein catabolism	

(continued on next page)

Table 1 (*continued*)

Gene name	Protein name	Spot no.	Accession no.	*p*-value	Fold change	MW	Seq. coverage	Cellular localization	Function	Reference (anxiety or depression)
Nucleotide metabolism										
ATIC	5-Aminoimidazole-4-carboxamide ribonucleotide formyltransferase/IMP cyclohydrolase	1147	Q9CWJ9	0.01	−1.06	64,200	19.3	Cytoplasm, mitochondria	Purine biosynthesis	
CMPK1	Cytidine monophosphate (UMP–CMP) kinase 1, cytosolic	3418	Q9DBP5	0.026	−1.23	22,148	42.9	Cytoplasm, nucleus, extracellular space	UDP/CDP formation from UMP/CMP	
HMGB1	Similar to High mobility group protein 1 (HMG-1)	3168	P63158	2.7E−05	−9.07	21,877	33.5	Nucleus	Nucleotide metabolism	(Lange et al., 2008; Najima et al., 2005) M
MTHFD1	Methylenetetrahydrofolate dehydrogenase (NADP+ dependent) 1	316	Q922D8	0.035	1.08	101,240	27.6	Mitochondria	One carbon metabolism	
Haem and lipid metabolism										
BLVRA	Biliverdin reductase A	2675	Q9CY64	1.7E−05	1.95	33,507	41.7	Cytoplasm	Stress response, haem metabolism	(Ewing and Maines, 2006; De Berardis et al., 2008) M/HD
ECHS1	Enoyl coenzyme A hydratase, short chain, 1, mitochondrial	3198	Q8BH95	0.035	1.13	31,457	37.9	Mitochondria	Fatty acid oxidation	
IDH1	Isocitrate dehydrogenase 1 (NADP+), soluble	2031	O88844	7.00E−06	2.60	46,644	50.2	Cytosol, mitochondria	Lipid metabolism	
OXCT1	3-Oxoacid CoA transferase 1	1533	Q9D0K2	0.00018	1.24	55,972	24	Extracellular space, mitochondria	Lipid metabolism	
PITPNA	Phosphatidylinositol transfer protein, alpha	2761	P16466, P53810	0.037	−1.14	31,889	53.1	Cytoplasm	Visual perception, lipid metabolism	(Desrumaux et al., 2005) M
SPR	Sepiapterin reductase	3221	Q64105	0.00063	−1.24	27,866	51	Cytoplasm	Tetrahydrobiopterin synthesis	(Thöny et al., 2000)
Protein biosynthesis and folding										
CAPZA1	Capping protein (actin filament) muscle Z-line, alpha 1	2477	P47753	0.033	−1.35	32,922	16.8	Cytoplasm	Chaperon protein folding	(Ewing and Maines, 2006)
CAPZA2	Capping protein (actin filament) muscle Z-line, alpha 2	2561	P47754, Q3T1K5	0.0061	−1.08	32,949	59.8	Cytoplasm	Chaperon protein folding	
CCT6A	Chaperonin containing TCP1, subunit 6A (zeta 1)	1242	P80317	0.0028	−1.1	57,987	19.4	Cytoplasm	Protein folding	
EIF4E	Eukaryotic translation initiation factor 4E	3275	P63073, P63074	1.20E−09	−11.42	25,035	27.6	Cytoplasm	Translation initiation	(Banko et al., 2007) M
ERP29	Endoplasmic reticulum protein 29	3275	P57759	1.20E−09	−11.42	28,807	39.3	Endoplasmic reticulum	Protein folding	

HSPA5	Heat shock 70 kDa protein 5 (glucose-regulated protein, 78 kDa)	704	P06761,	0.032	1.12	72,330	23.9	Cytoplasm	Stress response, protein folding	(Matigian et al., 2007) HD
Cytoskeletal proteins										
CAP1	CAP, adenylate cyclase-associated protein 1 (yeast)	704	P40124	0.032	1.12	72,330	23.9	Cytoplasm, plasma membrane	Signal transduction, cytoskeleton organization	(Nakatani et al., 2007) M/HD
CNP	2′,3′-Cyclic nucleotide 3′ phosphodiesterase	1989	P16330	0.03	−1.47	47,107	23.8	Cytoplasm, plasma membrane	Microtubule binding	(Brown et al., 1988) HD
EZR	Ezrin	654	P26040	0.00057	1.15	69,391	28.3	Cytoplasm, cytosol	Regulation of actin cytoskeleton	
LMNA	Lamin A/C	1097	P48678	0.00029	−1.71	74,221	19.5	Nucleus	Nuclear lamina formation	
SEPT4	Septin 4	1606	P28661	0.042	1.08	54,918	23	Cytoplasm, mitochondria, nucleus	Cytoskeleton organization, membrane organization vesicle targeting	
SEPT8	Septin 8	1606	Q8CHH9	0.042	1.08	49,794	25.9	Septin complex	Cytoskeleton organization, membrane organization vesicle targeting	
Brain development and neurogenesis										
DPYSL2	Dihydropyrimidinase-like 2	805	O08553	0.01	1.23	62,260	22.2	Cytoplasm, mitochondria	Neuronal development	(Beasley et al., 2006) HD
DPYSL3	Dihydropyrimidinase-like 3	1190	Q62188	0.026	−1.12	61,919	28.8	Cytoplasm	Axonal guidance	
PAK2	p21 (CDKN1A)-activated kinase 2	1307	P52480	0.00061	−1.14	57,827	28.2	Cytoplasm, membrane, nucleus	Signal transduction, neurite outgrowth	
Oxidative stress										
GLRX3	Glutaredoxin 3	2217	Q9CQM9	0.01	1.1	37,760	56.7	Cytoplasm	Redox homeostasis	
GSTM1	Glutathione S-transferase M1	3281	P10649	0.01	−1.18	25,954	61.5	Plasma membrane	Oxidative stress, prevention of cellular degeneration	
PRDX6	Peroxiredoxin 6	3090	O08709	0.0001	3.76	24,854	77.2	Endoplasmic reticulum	Oxidative stress	(Tsaluchidu et al., 2008) HD
QDPR	Quinoid dihydropteridine reductase	3140	Q8BVI4	3.60E−06	1.86	25,552	35.3	Cytoplasm	Metabolism, redox homeostasis	(Miller, 2008) HD
SIRT2	Sirtuin 2	2412	Q8VDQ8	0.02	−1.22	43,239	45.5	Cytoplasm, nucleus	Regulation of transcription, DNA-dependent, redox homeostasis	(Pollak et al., 2005) M

(continued on next page)

Table 1 (*continued*)

Gene name	Protein name	Spot no.	Accession no.	*p*-value	Fold change	MW	Seq. coverage	Cellular localization	Function	Reference (anxiety or depression)
Signal transduction										
MAP2K6	Mitogen activated protein kinase kinase 6	317	P70236	0.023	−1.13	37,412	37.1	Cytoplasm	Signal transduction	(Pawlak et al., 2003; Duman et al., 2008) M
PPP1CA	Protein phosphatase 1, catalytic subunit, alpha isoform	2473	P62137	0.0064	−1.19	37,524	27.3	Nucleus, cytoplasm	Metabolism, cytokinesis, signaling	(Skelton et al., 2003) M
PPP2R2A	Protein phosphatase 2 (formerly 2A), regulatory subunit B, alpha isoform	1726	P36876	0.039	−1.05	51,661	17.4	Cytoplasm	Signal transduction	(Beaulieu et al., 2008) M
TARDBP	TAR DNA binding protein	1996	Q921F2	7.00E−05	−1.37	44,529	27.3	Nucleus	Transcription regulation	
YWHAH	Tyrosine 3-monooxygenase/ tryptophan 5-monooxygenase activation protein	2453	P68510, P68511	0.026	−1.22	28,194	34.6	Cytoplasm	Signal transduction	(Altar et al., 2009)
Miscellaneous										
ALDH2	Aldehyde dehydrogenase 2 family (mitochondrial)	1646	P47738	0.037	−1.14	31,889	53.1	Mitochondria	Alcohol metabolism	(Huang et al., 2004) HD
CA2	Carbonic anhydrase II	3121	P00920	0.0063	1.17	29,015	49.6	Cytoplasm, plasma membrane	One carbon metabolism	(Beasley et al., 2006) HD
DDX3X	DEAD (Asp-Glu-Ala-Asp) box polypeptide 3, X-linked	837	Q62167	0.00054	1.22	73,085	38.8	Cytoplasm, nucleus	RNA helicase, translation initiation, splicing	
DNM1	Dynamin 1	321	P21575	0.0062	−1.76	97,280	21.6	Cytoplasm, cytoskeleton	Endocytosis	

DNM1L	Dynamin 1-like	569	O35303, Q8K1M6	0.026	−1.2	83,892	25.6	Cytoplasm, mitochondria	Regulation of mitochondrial morphology	
HGS	Hepatocyte growth factor-regulated tyrosine kinase substrate	309	Q99LI8	0.0001	3.76	24,854	77.2	Cytosol, cytoplasma, membrane	Signal transduction, endocytosis	
HNRNPH1	Heterogeneous nuclear ribonucleoprotein H1 (H)	1614	O35737	0.015	1.21	49,182	27.4	Nucleus	RNA processing	
HNRPDL	Heterogeneous nuclear ribonucleoprotein D-like	2540	Q3SWU3	0.041	−1.1	35,227	31.1	Cytoplasm, nucleus	RNA metabolism	
IMMT	Inner membrane protein, mitochondrial (mitofilin)	869	Q8CAQ8	0.049	−1.06	83,883	34.9	Mitochondria	Mitochondrial inner membrane morphogenesis	
NSFL1C	NSFL1 (p97) cofactor (p47)	1941	O35987, Q9CZ44	1.90E−05	−1.75	40,662	31.9	Nucleus	Membrane fusion	
PCBP1	Poly(rC) binding protein 1	2364	P60335	0.048	1.2	37,480	19.4	Cytoplasm, nucleus	mRNA metabolism	
PCMT1	Protein-L-isoaspartate (D-aspartate) O-methyltransferase	3305	P22062, P23506	0.00055	1.32	24,624	47.6	Cytoplasm	Protein modification	(Ikegaya et al., 2001) M
PRPF19	PRP19/PSO4 pre-mRNA processing factor 19 homolog (*S. cerevisiae*)	1490	Q99KP6	0.035	−1.1	55,221	13.1	Cytoplasm, nucleus	DNA repair	
SCRN1	Secernin 1	1687	Q9CZC8	0.026	1.12	46,308	51.9	Cytoplasm, nucleus	Exocytosis	
VDAC2	Voltage-dependent anion channel 2	2895	P81155, Q60930	0.045	−1.05	31,729	35.6	Mitochondria	Apoptosis regulation	

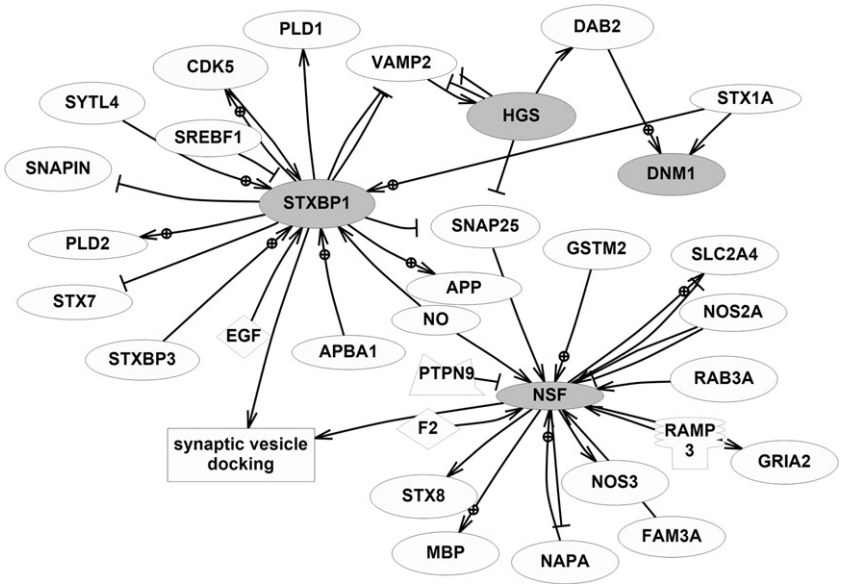

Figure 5 Proteins of synaptic docking (by gray) changed in AX mice. The network shows proteins directly coupled to the anxiety influenced proteins. Abbreviations: *gray*: DNM1 — dynamin 1, HGS — hepatocyte growth factor-regulated tyrosine kinase substrate, NSF — N-ethylmaleimide-sensitive factor, STXBP1 — syntaxin binding protein 1, *white labeled*: APBA1 — amyloid beta (A4) precursor protein binding, family A, member 1, APP — amyloid beta (A4) precursor protein (peptidase nexin-II, Alzheimer disease), CDK5 — cyclin-dependent kinase 5, DAB2 — disabled homolog 2, mitogen-responsive phosphoprotein, EGF — epidermal growth factor, EGR1 — early growth response protein, F2 — coagulation factor II, FAM3A — family with sequence similarity 3, member A, GRIA2 — glutamate receptor, ionotropic, AMPA 2, GSTM2 — glutathione S-transferase M2 (muscle), MAPK1 — mitogen activated protein kinase 1, MBP — myelin basic protein, NAPA — N-ethylmaleimide-sensitive factor attachment protein, alpha, NO — nitric oxide, NOS2A — nitric oxide synthase 2A (inducible, hepatocytes), NOS3 — nitric oxide synthase 3 (endothelial cell), PLD1 — phospholipase D1, PLD2 — phospholipase D2, PTPN9 — protein tyrosine phosphatase, non-receptor type 9, RAB3A — RAB3A, member RAS oncogene family, RAMP3 — receptor (G protein-coupled) activity modifying protein 3, SLC2A4 — solute carrier family 2 (facilitated glucose transporter), member 4, SNAP25 — synaptosomal-associated protein, 25 kDa, SNAPIN — SNAP-associated protein, SREBF1 — sterol regulatory element-binding transcription factor 1, STX1A — syntaxin 1A (brain), STX7 — syntaxin 7, STX8 — syntaxin 8, SYTL4 synaptotagmin-like 4 (granuphilin-a), and VAMP2 — vesicle-associated.

proteins we revealed has connection to brain-derived neurotrophic factor (BDNF), a factor responsible for proliferation of the granule cells in the hippocampus after antidepressant treatment (Martinowich et al., 2007).

The metabolic systems of the brain tissue also changed in AX mice (see Supplementary material). We found changes in the concentration of proteins that were involved in carbohydrate metabolism, protein and amino acid metabolism and nucleic acid metabolism. The direction of changes and the location of the altered proteins within the metabolic protein networks do not point to so extreme metabolite concentration changes in anxiety as in hypoxia. On the other hand, it is known that minor alterations in carbohydrate metabolism can have an effect on cognitive functions (Fowler, 1997). The influenced metabolic pathways of the brain metabolism demonstrated in our study could provide useful new putative targets for the search of additional biomarkers in anxiety disorders (Ditzen et al., 2006, 2009).

5. Conclusion

In conclusion, we developed an inbred mouse strain that displays the stress symptoms that are relevant to human anxiety disorders on the basis of regular anxiety tests. This mouse strain could prove to be a useful tool for pharmacological research. A proteomics study on the whole-brain homogenate revealed extensive changes in the proteome of AX mice, which included changes in proteins involved in either serotonin receptor protein packets, metabolic events, oxidative stress, synaptic docking or signal transduction pathways. We reproduced the previously known changes in glyoxalase, which is considered to be an anxiety biomarker in mice. Protein changes suggest modulation of many different major functional protein networks of brain cells. Our data support that whole-brain proteomics allows a reliable characterization of animal models of psychiatric disorders at molecular level, thus providing estimates of overlapping between human and mouse anxiety. The model is highly suitable for molecular studies because of the homogeneity of its phenotype.

Role of the funding source

This work was supported by the National Office for Research and Technology (NKTH), GVOP-3.2.1.-2004-04-0309, DNT/RET and CellKom/RET, Hungary. NKTH had no further role in the study design; in the collection, analysis and interpretation of data; in the

writing of the report; and in the decision to submit the paper for publication.

Contributors

Éva M. Szegő designed the study and made the proteomics experiments, Tamás Janáky, Zoltán Szabó and Attila Csorba contributed to the Mass Spect. experiments, Hajnalka Kompagne and Géza Müller made the behavioral experiments, György Lévay designed the behavioral experiments, Attila Simor managed the literature searches and analyses, Gábor Juhász designed the study and wrote the first draft of the manuscript, and Katalin A. Kékesi designed the study, contributed to proteomics analyses and wrote the manuscript. All authors contributed to and have approved the final manuscript.

Conflict of interest

All authors declare that they have no conflicts of interest.

Acknowledgement

The present study was supported by GVOP-3.2.1.-2004-04-0309, DNK RET and Cellkom RET grants. We are grateful to Cathy Ludwig, András Czurkó and Zoltán Janka for helpful discussion and for improving the quality of the manuscript.

Appendix A. Supplementary data

The Supplementary material accompanying this article is available at doi:10.1016/j.euroneuro.2009.11.003.

References

Abi-Dargham, A., Charney, D.S., Krystal, J.H., 1997. Benzodiazepin receptor antagonists. Possible uses in treatment of neuropsychiatric disorders. CNS Drugs 8, 244–256.

Ackermann, T.F., Hörtnagl, H., Wolfer, D.P., Colacicco, G., Sohr, R., Lang, F., Hellweg, R., Lang, U.E., 2008. Phosphatidylinositide dependent kinase deficiency increases anxiety and decreases GABA and serotonin abundance in the amygdale. Cell. Physiol. Biochem. 22, 735–744.

Agid, Y.G., Buzsaki, D.M., Diamond, R., Frackowiak, J., Giedd, J., Girault, J.A., Grace, A., Lambert, J.J.Manji, Mayberg, H., Popoli, M., Prochiantz, A., Richter-Levin, G., Somogyi, P., Spedding, M., Svenningsson, P., Weinberger, D., 2007. How can drug discovery for psychiatric disorders be improved? Nat. Rev. 6, 189–201.

Al-Damluji, S., 2004. The mechanism of action of antidepressants: a unitary hypothesis based on transport-p. Curr. Drug Targets CNS Neurol. Disord. 3, 201–216.

Altar, C.A., Vawter, M.P., Ginsberg, S.D., 2009. Target identification for CNS diseases by transcriptional profiling. Neuropsychopharmacology 34, 18–54.

Bachmann, R.F., Schloesser, R.J., Gould, T.D., Manji, H.K., 2005. Mood stabilizers target cellular plasticity and resilience cascades: implications for the development of novel therapeutics. Mol. Neurobiol. 32, 173–202.

Banko, J.L., Merhav, M., Stern, E., Sonenberg, N., Rosenblum, K., Klann, E., 2007. Behavioral alterations in mice lacking the translation repressor 4E-BP2. Neurobiol. Learn. Mem. 87, 248–256.

Bayés, A., Grant, S.G., 2009. Neuroproteomics: understanding the molecular organization and complexity of the brain. Nat. Rev. Neurosci. 10, 635–646.

Beasley, C.L., Pennington, K., Behan, A., Wait, R., Dunn, M.J., Cotter, D., 2006. Proteomic analysis of the anterior cingulate cortex in the major psychiatric disorders: evidence for disease-associated changes. Proteomics 6, 3414–3425.

Beaulieu, J.M., Marion, S., Rodriquiz, R.M., Medvedev, I.O., Sotnikova, T.D., Ghisi, V., Wetsel, W.C., Lefkowitz, R.J., Gainetdinov, R.R., Caron, M.G., 2008. A beta-arrestin 2 signaling complex mediates lithium action on behavior. Cell 132, 125–136.

Borsini, F., Podhorna, J., Marazziti, D., 2002. Do animal models of anxiety predict anxiolytic-like effects of antidepressants? Psychopharmacology 163, 121–141.

Bourin, M., Hascoet, M., 2001. Drug mechanisms in anxiety. Curr. Opin. Investig. Drugs 2, 259–265.

Bourin, M., Petit-Demoulière, B., Dhonnchadha, B.N., Hascöet, M., 2007. Animal models of anxiety in mice. Fundam. Clin. Pharmacol. 21, 567–574.

Brown, S.L., Charney, D.S., Woods, S.W., Heninger, G.R., Tallman, J., 1988. Lymphocyte beta-adrenergic receptor binding in panic disorder. Psychopharmacology (Berlin) 94, 24–28.

Cabral, A., Ross, J.D., Castilho, V.M., Brandao, M.L., Nobre, M.J., 2009. Glutamate receptor antagonism in inferior colliculus attenuates elevated startle response of high anxiety diazepam-withdrawn rats. Neuroscience 161, 707–717.

Carboni, L., Piubelli, C., Pozzato, C., Astner, H., Arban, R., Righetti, P.G., Hamdan, M., Domenici, E., 2006a. Proteomic analysis of rat hippocampus after repeated psychosocial stress. Neuroscience 137, 1237–1246.

Carboni, L., Vighini, M., Piubelli, C., Castelletti, L., Milli, A., Domenici, E., 2006b. Proteomic analysis of rat hippocampus and frontal cortex after chronic treatment with fluoxetine or putative novel antidepressants: CRF1 and NK1 receptor antagonists. Eur. Neuropsychopharmacol. 16, 521–537.

Carroll, M., Dyer, J., Sossin, W.S., 2006. Serotonin increases phosphorylation of synaptic 4EBP through TOR, but eukaryotic initiation factor 4E levels do not limit somatic cap-dependent translation in aplysia neurons. Mol. Cell. Biol. 26, 8586–8598.

Choudary, P.V., Molnar, M., Evans, S.J., Tomita, H., Li, J.Z., Vawter, M.P., Myers, R.M., Bunney Jr., W.E., Akil, H., Watson, S.J., Jones, E.G., 2005. Altered cortical glutamatergic and GABAergic signal transmission with glial involvement in depression. Proc. Natl. Acad. Sci. U. S. A. 102, 15653–15658.

Covault, J., Pettinati, H., Moak, D., Mueller, T., Kranzler, H.R., 2004. Association of a long-chain fatty acid-CoA ligase 4 gene polymorphism with depression and with enhanced niacin-induced dermal erythema. Am. J. Med. Genet. B. Neuropsychiatr. Genet. 127B, 42–47.

De Berardis, D., Conti, C.M., Campanella, D., Carano, A., Di Giuseppe, B., Valchera, A., Tancredi, L., Serroni, N., Pizzorno, A.M., Fulcheri, M., Gambi, F., Sepede, G., Moschetta, F.S., Salerno, R.M., Ferro, F.M., 2008. Evaluation of plasma antioxidant levels during different phases of illness in adult patients with bipolar disorder. J. Biol. Regul. Homeost. Agents 22, 195–200.

Desrumaux, C., Risold, P.Y., Schroeder, H., Deckert, V., Masson, D., Athias, A., Laplanche, H., Le Guern, N., Blache, D., Jiang, X.C., Tall, A.R., Desor, D., Lagrost, L., 2005. Phospholipid transfer protein (PLTP) deficiency reduces brain vitamin E content and increases anxiety in mice. FASEB 19, 296–297.

Ditzen, C., Jastorff, A.M., Kessler, M.S., Bunck, M., Teplytska, L., Erhardt, A., Krömer, S.A., Varadarajulu, J., Targosz, B.S., Sayan-Ayata, E.F., Holsboer, F., Landgraf, R., Turck, C.W., 2006. Protein biomarkers in a mouse model of extremes in trait anxiety. Mol. Cell Proteomics 5, 1914–1920.

Ditzen, C., Varadarajulu, J., Czibere, L., Gonik, M., Targosz, B.S., Hambsch, B., 2009. Proteomic-based genotyping in a mouse model of trait anxiety exposes disease-relevant pathways. Mol. Psychiatry 1–10 (2009 Jan 13).

Duman, C.H., Schlesinger, L., Russell, D.S., Duman, R.S., 2008. Voluntary exercise produces antidepressant and anxiolytic behavioral effects in mice. Brain Res. 1199, 148–158.

Ewing, J.F., Maines, M.D., 2006. Regulation and expression of heme oxygenase enzymes in aged-rat brain: age related depression in HO-1 and HO-2 expression and altered stress-response. J. Neural Transm. 113, 439–454.

Fernández, E., Collins, M.O., Uren, R.T., Kopanitsa, M.V., Komiyama, N.H., Croning, M.D.R., Zografos, L., Armstrong, J.D., Choudhary, J.S., Grant, S.G.N., 2009. Targeted tandem affinity purification of PSD-95 recovers core postsynaptic complexes and schizophrenia susceptibility proteins. Mol. Sys. Biol. 5, 1–17.

Fowler, V.M., 1997. Capping actin filament growth: tropomodulin in muscle and nonmuscle cells. Soc. Gen. Physiol. Ser. 52, 79–89.

Garcia-Garcia, A.L., Elizalde, N., Matrov, D., Harro, J., Wojcik, S.M., Venzala, E., Ramirey, M.J., Del Rio, J., Tordera, R.M., 2009. Increased vulnerability to depressive-like behavior of mice with decreased expression of VGLUT1. Biol. Psychiatry 66, 275–282.

Garner, M., Möhler, H., Stein, D.J., Mueggler, T., Baldwin, D.S., 2009. Research in anxiety disorders: from the bench to the bedside. Eur. Neuropsychopharmacol. 19, 381–390.

Gisler, S.M., Kittanakom, S., Fuster, D., Wong, V., Bertic, M., Radanovic, T., Hall, R.A., Murer, H., Biber, J., Markovich, D., Moe, O.W., Stagljar, I., 2008. Monitoring protein–protein interactions between the mammalian integral membrane transporters and PDZ-interacting partners using a modified split-ubiquitin membrane yeast two-hybrid system. Mol. Cell. Prot. 7, 1362–1377.

Graeff, F.G., Guimaraes, F.S., De Andrade, T.G.C.S., Deakin, J.F. W., 1996. Role of 5-HT in stress, anxiety and depression. Pharmacol. Biochem. Behav. 54, 129–141.

Hahn, C., Banerjee, A., MacDonald, M.L., Cho, D., Kamins, J., Nie, Z., Borgmann-Winter, K.E., Grosser, T., Pizarro, A., Ciccimaro, E., Arnold, S.E., Wang, H., Blair, I.A., 2009. The post-synaptic density of human postmortem brain tissues: an experimental study paradigm for neuropsychiatric illnesses. PlosOne 4, e5251.

Handley, S.L., McBlane, J.W., 1993. 5-HT drugs in animal models of anxiety. Psychopharmacology (Berlin) 112, 13–20.

Holtmaat, A., Svoboda, K., 2009. Experience-dependent structural synaptic plasticity in the mammalian brain. Nat. Rev. Neurosci. 10, 647–658.

Hovatta, I., Tennant, R.S., Helton, R., Marr, R.A., Singer, O., Redwine, J.M., Ellison, J.A., Schadt, E.E., Verma, I.M., Lockhart, D.J., Barlow, C., 2005. Glyoxalase 1 and glutathione reductase 1 regulate anxiety in mice. Nature 438, 662–666.

Huang, S.Y., Lin, W.W., Ko, H.C., Lee, J.F., Wang, T.J., Chou, Y.H., Yin, S.J., Lu, R.B., 2004. Possible interaction of alcohol dehydrogenase and aldehyde dehydrogenase genes with the dopamine D2 receptor gene in anxiety-depressive alcohol dependence. Alcohol. Clin. Exp. Res. 28, 374–384.

Ikegaya, Y., Yamada, M., Fukuda, T., Kuroyanagi, H., Shirasawa, T., Nishiyama, N., 2001. Aberrant synaptic transmission in the hippocampal CA3 region and cognitive deterioration in protein-repair enzyme-deficient mice. Hippocampus 11, 287–298.

Johnson, P.L., Truitt, W.A., Fitz, S.D., Lowry, C.A., Shekhar, A., 2008. Neural pathways underlying lactate-induced panic. Neuropsychopharmacology 33, 2093–2107.

Johnston-Wilson, N.L., Sims, C.D., Hofmann, J.P., Anderson, L., Shore, A.D., Torrey, E.F., Yolken, R.H., 2000. Disease-specific alterations in frontal cortex brain proteins in schizophrenia, bipolar disorder, and major depressive disorder. The Stanley Neuropathology Consortium. Mol. Psychiatr. 5, 142–149.

Kalueff, A.V., Murphy, D.L., 2007. The importance of cognitive phenotypes in experimental modeling of animal anxiety and depression. Neural Plast. 2007, 52087.

Khawaja, X., Xu, J., Liang, J.J., Barrett, J.E., 2004. Proteomic analysis of protein changes developing in rat hippocampus after chronic antidepressant treatment: implications for depressive disorders and future therapies. J. Neurosci. Res. 75, 451–460.

King, J.S., Teo, R., Ryves, J., Reddy, J.V., Peters, O., Orabi, B., Hoeller, O., Williams, R.S., Harwood, A.J., 2009. The mood stabiliser lithium suppresses PIP3 signalling in *Dictyostelium* and human cells. Dis. Model Mech. 2, 306–312.

Kishida, K.T., Klann, E., 2007. Sources and targets of reactive oxygen species in synaptic plasticity and memory. Antioxid. Redox Signal. 9, 233–244.

Krömer, S.A., Kessler, M.S., Milfay, D., Birg, I.N., Bunck, M., Czibere, L., Panhuysen, M., Pütz, B., Deussing, J.M., Holsboer, F., Landgraf, R., Turck, C.W., 2005. Identification of glyoxalase-I as a protein marker in a mouse model of extremes in trait anxiety. J. Neurosci. 25, 4375–4384.

Lange, S.S., Mitchell, D.L., Vasquez, K.M., 2008. High mobility group protein B1 enhances DNA repair and chromatin modification after DNA damage. Proc. Natl. Acad. Sci. U. S. A. 105, 10320–10325.

Lowry, C.A., Hale, M.W., Evans, A.K., Heerkens, J., Staub, D.R., Gasser, P.J., Shekhar, A., 2008. Serotoninergic systems, anxiety, and affective disorder: focus on the dorsomedial part of the dorsal raphe nucleus. Ann. N. Y. Acad. Sci. 1148, 86–94.

Martinowich, K., Manji, H., Lu, B., 2007. New insights into BDNF function in depression and anxiety. Nat. Neurosci. 10, 1089–1093.

Matigian, N., Windus, L., Smith, H., Filippich, C., Pantelis, C., McGrath, J., Mowry, B., Hayward, N., 2007. Expression profiling in monozygotic twins discordant for bipolar disorder reveals dysregulation of the WNT signaling pathway. Mol. Psychiatry 12, 815–825.

Miller, A.L., 2008. The methylation, neurotransmitter, and antioxidant connections between folate and depression. Altern. Med. Rev. 13, 216–226.

Miller, D.B., O'Callaghan, J.P., 2005. Depression, cytokines, and glial function. Metabolism 54, 33–38.

Najima, Y., Yahagi, N., Takeuchi, Y., Matsuzaka, T., Sekiya, M., Nakagawa, Y., Amemiya-Kudo, M., Okazaki, H., Okazaki, S., Tamura, Y., Iizuka, Y., Ohashi, K., Harada, K., Gotoda, T., Nagai, R., Kadowaki, T., Ishibashi, S., Yamada, N., Osuga, J., Shimano, H., 2005. High mobility group protein-B1 interacts with sterol regulatory element-binding proteins to enhance their DNA binding. J. Biol. Chem. 280, 27523–27532.

Nakatani, N., Ohnishi, T., Iwamoto, K., Watanabe, A., Iwayama, Y., Yamashita, S., Ishitsuka, Y., Moriyama, K., Nakajima, M., Tatebayashi, Y., Akiyama, H., Higuchi, T., Kato, T., Yoshikawa, T., 2007. Expression analysis of actin-related genes as an underlying mechanism for mood disorders. Biochem. Biophys. Res. Commun. 352, 780–786.

Nishikawa, H., Inoue, T., Masui, T., Izumi, T., Nakagawa, S., Koyama, T., 2008. Pharmacokinetic interaction between tandospirone and fluvoxamine in the rat contextual conditioned fear stress model and its functional consequence: involvement of cytochrome P450 3A4. Psychiatry Clin. Neurosci. 62, 591–596.

Otomo, M., Takahashi, K., Miyoshi, H., Osada, K., Nakashima, H., Yamaguchi, N., 2008. Some selective serotonin reuptake inhibitors inhibit dynamin I guanosine triphosphatase (GTPase). Biol. Pharm. Bull. 31, 1489–1495.

Pawlak, R., Magarinos, A., Melchor, J., McEwen, B., Strickland, S., 2003. Tissue plasminogen activator in the amygdale is critical for stress-induced anxiety-like behavior. Nat. Neurosci. 6, 168–174.

Pollak, D., Weitzdoerfer, R., Yang, Y.W., Prast, H., Hoeger, H., Lubec, G., 2005. Cerebellar protein expression in three different mouse strains and their relevance for motor performance. Neurochem. Int. 46, 19–29.

Scoles, D.R., 2008. The merlin interacting proteins reveal multiple targets for NF2 therapy. Biochim. Biophys. Acta 1785, 32–54.

Shevchenko, A., Wilm, M., Vorm, O., Mann, M., 1996. Mass spectrometric sequencing of proteins silver-stained polyacrylamide gels. Anal. Chem. 68, 850–858.

Skelton, M.R., Ponniah, S., Wang, D.Z., Doetschman, T., Vorhees, C.V., Pallen, C.J., 2003. Protein tyrosine phosphatase alpha (PTP alpha) knockout mice show deficits in Morris water maze learning, decreased locomotor activity, and decreases in anxiety. Brain Res. 984, 1–10.

Sousa, N., Lukoyanov, N.V., Madeira, M.D., Almeida, O.F.X., Paula-Barbosa, 2000. Reorganization of the morphology of hippocampal neurites and synapses after stress-induced damage correlates with behavioral improvement. Neuroscience 97, 253–266.

Sünram-Lea, S.I., Dewhurst, S.A., Foster, J.K., 2008. The effect of glucose administration on the recollection and familiarity components of recognition memory. Biol. Psychol. 77, 69–75.

Thöny, B., Auerbach, G., Blau, N., 2000. Tetrahydrobiopterin biosynthesis, regeneration and functions. Biochem. J. 347 (Pt 1), 1–16.

Tohda, C., Nakanishi, R., Kadowaki, M., 2009. Hyperactivity, memory deficit and anxiety-related behaviors in mice lacking the p85alpha subunit of phosphoinositide-3 kinase. Brain Dev. 31, 69–74.

Toro, C., Deakin, J.F., 2005. NMDA receptor subunit NRI and postsynaptic protein PSD-95 in hippocampus and orbitofrontal cortex in schizophrenia and mood disorder. Schizophr. Res. 80, 323–330.

Tsaluchidu, S., Cocchi, M., Tonello, L., Puri, B.K., 2008. Fatty acids and oxidative stress in psychiatric disorders. BMC Psychiatry 8 (Suppl. 1), S5.

Tyeryar, K.R., Undie, A.S., 2007. Tandem regulation of phosphoinositide signaling and acute behavioral effects induced by antidepressant agents in rats. Psychopharmacology (Berlin) 193, 271–282.

Tyeryar, K.R., Vongtau, H.O., Undieh, A.S., 2008. Diverse antidepressants increase CDP-diacylglycerol production and phosphatidylinositide resynthesis in depression-relevant regions of the rat brain. BMC Neurosci. 24, 9–12.

Uys, J.D., Stein, D.J., Daniels, W.M., 2006. Neuroproteomics: relevance to anxiety disorders. Curr. Psychiatry Rep. 8, 286–290.

van Zundert, B., Yoshii, A., Constantine-Paton, M., 2004. Receptor compartmentalization and trafficking at glutamate synapses: a developmental proposal. Trends Neurosci. 27, 428–437.

Wand, G., 2005. The anxious amygdala: CREB signaling and predisposition to anxiety and alcoholism. J. Clin. Invest. 115, 2697–2699.

Weder, H.G., 1978. The interaction of central acting drugs with glutamate dehydrogenase. Arzneimittelforschung 28, 752–755.

Wu, L.J., Kim, S.S., Zhuo, M., 2008. Molecular targets of anxiety: from membrane to nucleus. Neurochem. Res. 33, 1925–1932.

Zarate Jr., C.A., Singh, J., Manji, H.K., 2006. Cellular plasticity cascades: targets for the development of novel therapeutics for bipolar disorder. Biol. Psychiatry 59, 1006–1020.